JOURNAL OF SOLID STATE CHEMISTRY 92, 520–530 (1991)

On the Crystal Structure of $KInS_2$-I

C. K. LOWE-MA, D.O. KIPP, AND T. A. VANDERAH

Chemistry Division, Research Department, Naval Weapons Center, China Lake, California 93555

Received August 27, 1990; in revised form February 6, 1991

The ambient-pressure form of $KInS_2$ crystallizes in the monoclinic space group $C2/c$; a = 10.981(3), b = 10.979(3), c = 15.010(5) Å, β = 100.55(2)°, Vol = 1779.2(9) Å^3, Z = 16, D_x = 3.257 g/cm^3 for M_F = 218.04. An X-ray single-crystal structure determination has confirmed that $KInS_2$-I has the $TlGaSe_2$ structure. The bonding in $KInS_2$-I is highly covalent and exhibits both two-dimensional and three-dimensional features. The structure is comprised of layers of vertex-sharing $[In_4S_{10}]$ adamantane-like units composed of four $[InS_4]$ tetrahedra. The stacking arrangement of these layers creates channels that contain the potassium ions in distorted trigonal prismatic sites that provide the three-dimensionality of the structure. The strength of the interlayer potassium–sulfur bonding is reflected in the nonmicaceous morphology and water-stability of the transparent light-yellow crystals.

Introduction

Our investigation of ternary indium sulfide systems was undertaken to identify new compounds for possible applications as optical ceramics and to confirm reported structures and structural interrelationships. In a series of crystal growth experiments using eutectic halide fluxes (*1*), large numbers of high-quality platelets and rods of the compound $KInS_2$ were obtained. We became interested in the polymorphism reported for this composition and the related versatility of trivalent indium, namely, tetrahedral versus octahedral coordination. This coordinative versatility plays a significant role in determining infrared optical properties.

Three polymorphs of $KInS_2$ have been previously identified—one ambient-pressure form ($KInS_2$-I) (*2*) and two high-pressure forms ($KInS_2$-II and -III) (*3*). Although, to our knowledge, full single-crystal structure determinations have not been reported for any of the polymorphs, possible structures have been deduced from studies of polycrystalline samples. $KInS_2$-I is reportedly isostructural with ambient-pressure $RbInS_2$-I and $TlGaSe_2$ (*2, 4*) and crystallizes with monoclinic lattice symmetry (a = 15.64, b = 10.88, c = 11.16 Å; β = 103°) (*2*); this structure type features tetrahedral coordination of the trivalent cations while the larger monovalent ions occupy trigonal prisms (*5*). $KInS_2$-I transforms to two other higher density polymorphs at elevated pressures and temperatures. $KInS_2$-II (30 kbar, 1000°C) (*3*) is isostructural with TlSe ($Tl^ITl^{III}Se_2$) with a tetragonal unit cell ($I4/mcm$; a = 7.769(3), c = 6.672(3) Å) (*3*) and features chains of opposite-edge-shared $[InS_4]$ tetrahedra and eight-coordinate potassium in square antiprismatic sites. $KInS_2$-III (20 kbar, 350°C) (*3*) exhibits the α-$NaFeO_2$ structure with a hexagonal unit cell (a =

0022-4596/91 $3.00

3.875(2), c = 21.794(5) Å) (*3*). This structure is an ordered rock salt derivative; the coordination of both potassium and indium is octahedral with the two metals segregated on alternate (111) planes of the parent NaCl structure. $KInS_2$-II can be converted to $KInS_2$-III, the highest density phase, by application of 40 kbar pressure at 1000°C. Both high-pressure forms convert to $KInS_2$-I at ambient pressure above 300°C.

Limited information on the physical properties of the $KInS_2$ phases is available. $KInS_2$-I melts at 1024°C *in vacuo* and is stable in air below 380°C (*6*). A band gap of 3.0 eV was found for crystals of $KInS_2$-I (*7*). The infrared spectrum of $KInS_2$-I measured below 400 cm^{-1} indicated groups of absorption bands in the regions 350–290, 180–110, and below 100 cm^{-1} (*6*).

In the present study, a full X-ray single-crystal structure determination was carried out for $KInS_2$-I to elucidate details and confirm its relationship to the $TlGaSe_2$ structure (*5*).

Experimental

In previous studies, $KInS_2$-I was prepared as crystals from melts of S, K_2CO_3, and In_2O_3 (*2, 6*) or S, K, and In_2S_3 (*5*) at 800–1000°C and in powder form from $KInO_2$ or K_2CO_3 and In_2O_3 under H_2S at 600–800°C (*6*). In the present study, crystals of $KInS_2$-I were grown from KCl-containing eutectic halide fluxes as a coproduct of crystallization of compounds in the Ca–In–S and Sr–In–S systems (*1*). The crystallographic data reported here were obtained using crystals grown from a $CaCl_2$: KCl 25 : 75 mole% eutectic mixture (mp 600°C). To prepare the flux, $CaCl_2$ (Baker, reagent) and KCl (Baker reagent) were dried under vacuum at 150°C, weighed, ground together 5 min in air, and then dried again prior to use. The crystal growth charge consisted of an equimolar mixture of CaS (Cerac 4N) and In_2S_3 (AESAR 5N) ground together 5–10 min in air just prior to use. The flux : charge mass ratio of the crystal growth reaction mixture was 85 : 15. The experiment was carried out in a graphite crucible enclosed in a silica ampule; the double container was outgassed at 900°C under vacuum, cooled, and then quickly loaded with 5.3 g reaction mixture. The loaded ampules were held under dynamic vacuum at least 2.5 hr to obtain a pressure of less than 4×10^{-4} torr prior to sealing. The reaction mixture was heated in 16 hr to 1070°C, soaked 6 days, cooled in 48 hr to 930°C, heated in 7 hr to 1030°C, cooled at 1.25°/hr to 580°C, and then cooled to room temperature in 24 hr. Chemical attack on the interior ampule surfaces was minimal. Crystals were removed from the flux by leaching with distilled water. The very pale yellow-orange square platelets and rectangular rods of $KInS_2$-I, ranging from 0.1 to 3 mm in their longest dimension, had well-formed faces and were easily separated from the smaller whiskers of the alkaline-earth indium sulfides under a microscope. Semiquantitative elemental analyses were obtained with a scanning electron microscope by energy-dispersive X-ray spectroscopy (EDX) using an AMRAY 1400, TRACOR TN2000 analyzer. The results of multiple determinations were consistent with the stoichiometry $KInS_2$ for both the platelets and the rods; no incorporation of Ca, Sr, or Cl was detected in any of the crystals.

Unit cell parameters were obtained with a Nicolet R3 single-crystal diffractometer using monochromated Mo$K\alpha$. Unit cells were determined for two platelets [platelet 1: a = 10.978(3), b = 10.984(3), c = 15.015(5) Å, β = 100.53 (3)°; platelet 2: a = 10.981(3), b = 10.979 (3), c = 15.010(5) Å, β = 100.55(2)°] and a rod [a = 10.975(6), b = 10.999(7), c = 15.030(11) Å, β = 100.63(5)°]. The platelets and rod were all found to be C-centered monoclinic. Intensity data were obtained for pale yellow-orange platelet 2, approximate dimensions 0.02 × 0.11 × 0.24 mm, with a Nicolet R3

using monochromated Mo$K\alpha$ at 293 K; 25 computer-centered reflections were used for the symmetry-constrained least-squares determination of the unit cell. Intensity data were collected using the following parameters: $2\theta/\theta$ scans; 4–12°/min variable scan speed; scan width 2.0° plus $K\alpha$ separation; total background to total scan time ratio of 1.0; 2θ range of 4° to 60° (λ = 0.71073 Å); index ranges of $-16 \leq h \leq 16$, $0 \leq k \leq 16$, $-22 \leq l \leq 22$, with $h + k = 2n + 1$ not collected; three check reflections, (0,8,0), (0,0,10), (4,4,−1), collected every 93 reflections with most variation less than 3%. The data were corrected for Lorentz and polarization effects and, based on ψ - scans of 22 reflections, were empirically corrected for absorption assuming a lamellar model (minimum transmission of 0.52; maximum transmission of 0.95). Reflections with $h0l$, $h = 2n + 1$ and $l = 2n + 1$, and $00l$, $l = 2n + 1$ were absent, indicating space groups Cc or $C2/c$. In $C2/c$, R_{merge} = 0.035 for 2962 unique reflections; 1970 with $|F_o| \geq 3\sigma(F)$ were considered observed and used for structure solution and refinement.

Initial indium and sulfur atomic positions were obtained by Patterson methods followed by direct methods phase expansion. The remaining sulfur and potassium positions were obtained by Fourier cycling. After full-matrix least-squares minimization of $\sum w(F_o - kF_c)^2$ using neutral-atom scattering factors, R = 0.047 with anisotropic thermal parameters. At this point significant difference Fourier peaks were observed. The two strongest difference peaks were modeled as partially occupied indium sites based on the sulfur–unknown peak bond lengths. Additional weak difference peaks were also observed near the two sulfur atoms S(2) and S(5), near K(2), and near both indium atoms In(1) and In(2), although additional atoms at these difference peak positions were not included or refined. For 82 parameters, including two partially occupied (disordered) indium sites, full-matrix least-squares refinement, with weighting $w = 1/[\sigma^2(F) + 0.0008F^2]$, converged. For the final cycle, the largest and mean shift/e.s.d. ratios were 0.24 and 0.02, respectively, with R = 0.035, wR = 0.044, GOF = 1.04. Atomic coordinates and thermal parameters from the final cycle, including those for the disordered, partially occupied indium atoms In(3) and In(4), are given in Table I.[1] All calculations were accomplished using the SHELXTL PC package of programs (*8*).

Results

$KInS_2$-I is isostructural with $TlGaSe_2$ (*5*) and exhibits both two-dimensional and three-dimensional structural features. The structure consists of layers of vertex-sharing $[In_4S_{10}]$ adamantane-like units that are structurally analogous to vapor-phase P_4O_{10}; each $[In_4S_{10}]$ unit is comprised of four vertex-sharing $[InS_4]$ tetrahedra surrounding an empty octahedral site. One $[In_4S_{10}]$ unit is illustrated in Fig. 1 both as a ball-and-stick representation with thermal ellipsoids (1a) and as a polyhedral representation (1b). The In–S connections within one layer of $[In_4S_{10}]$ units are illustrated in Fig. 2. Vertex-sharing of the $[In_4S_{10}]$ units creates channels perpendicular to one another in the a–b plane that contain the potassium atoms. The layers of vertex-sharing $[In_4S_{10}]$ units stack perpendicular to c^* and each layer is related to the ones above and below by a two-fold rotation in the plane of a layer. The edges of the large $[In_4S_{10}]$ units

[1] See NAPS document No. 04856 for 9 pages of supplementary material. Order from ASIS/NAPS, Microfiche Publications, P.O. Box 3513, Grand Station, New York, NY 10163. Remit in advance $4.00 for microfiche copy or for photocopy $7.75 up to 20 pages plus $.30 for each additional page. All orders must be prepaid. Institutions and Organizations may order by purchase order. However, there is a billing and handling charge for this service of $15. Foreign orders add $4.50 for postage and handling, for the first 20 pages, and $1.00 for additional 10 pages of materials, $1.50 for postage of any microfiche orders.

TABLE I

ATOMIC COORDINATES AND THERMAL PARAMETERS ($Å^2$) FOR $KInS_2$-I

	x	y	z	U(eq)[a]
In(1)	0.39969(5)	−0.18817(6)	0.34473(5)	0.0144(1)
In(2)	0.14768(5)	0.06323(6)	0.34498(5)	0.0150(1)
K(1)	0.4663(2)	0.1875(2)	0.1162(1)	0.0343(5)
K(2)	0.2834(2)	0.4383(2)	0.3832(1)	0.0340(5)
S(1)	0.2591(2)	0.1927(3)	0.2506(1)	0.020(1)
S(2)	0.2983(2)	−0.0629(2)	0.4446(1)	0.033(1)
S(3)	0.5000	−0.0576(4)	0.2500	0.021(1)
S(4)	0.0	−0.0746(3)	0.2500	0.015(1)
S(5)	0.0490(2)	0.1876(2)	0.4461(1)	0.040(1)
In(3)[b]	0.4046(14)	0.3148(16)	0.3458(13)	0.020
In(4)[b]	0.3606(24)	0.0540(26)	0.1539(22)	0.020

	U_{11}[c]	U_{22}	U_{33}	U_{12}	U_{13}	U_{23}
In(1)	0.0139(2)	0.0144(2)	0.0151(2)	0.0031(1)	0.0036(1)	−0.0002(1)
In(2)	0.0140(2)	0.0150(2)	0.0158(2)	0.0033(1)	0.0024(1)	0.0005(1)
K(1)	0.0400(9)	0.0424(9)	0.0198(8)	−0.0232(8)	0.0034(5)	0.0004(6)
K(2)	0.0417(9)	0.0418(9)	0.0182(7)	0.0207(8)	0.0048(6)	0.0005(6)
S(1)	0.016(1)	0.015(1)	0.027(1)	−0.005(1)	0.005(1)	0.004(1)
S(2)	0.043(1)	0.045(1)	0.011(1)	0.033(1)	0.002(1)	0.000(1)
S(3)	0.019(1)	0.024(1)	0.022(1)	0.0	0.010(1)	0.0
S(4)	0.015(1)	0.006(1)	0.022(1)	0.0	0.000(1)	0.0
S(5)	0.050(1)	0.052(1)	0.017(1)	0.039(1)	0.004(1)	−0.001(1)

[a] Equivalent isotropic U defined as one-third of the trace of the orthogonalized U_{ij} tensor.

[b] Refinement of the partially occupied (disordered) atoms converged at occupancies of 0.041(2) for In(3) and at 0.025(2) for In(4).

[c] The form of the anisotropic thermal parameters is $-2\pi^2(h^2a^{*2}U_{11} + \ldots + 2klb^*c^*U_{23})$.

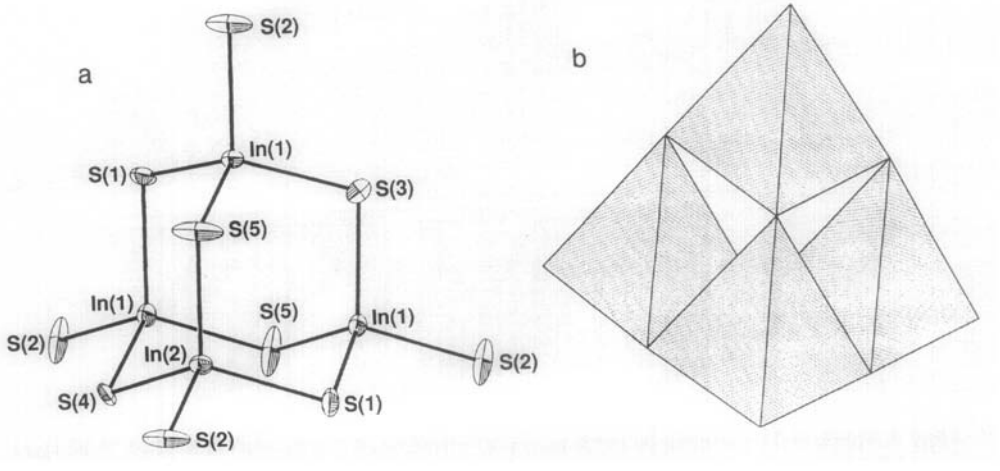

FIG. 1. Representations of the $[In_4S_{10}]$ unit in $KInS_2$-I. (a) Ball-and-stick plot with 50% probability thermal ellipsoids emphasizing the adamantane-like structure; (b) polyhedral plot emphasizing the analogy to vapor-phase P_4O_{10}.

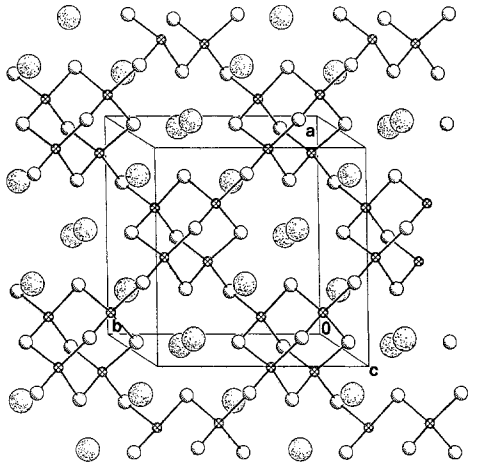

FIG. 2. Perspective view of one layer of $KInS_2$-I approximately along (001) illustrating the interconnections of the $[In_4S_{10}]$ units and the channels of potassium atoms.

in one layer nestle into the channels of the layers above and below as shown in Fig. 3, thus completing the trigonal prismatic coordination spheres about the potassiums.

As shown in Figs. 4a and 4b, each potassium is surrounded by six sulfurs in a distorted trigonal prism. The two crystallographically distinct potassiums alternate along each channel in trigonal prisms that share triangular faces. Polyhedral linkage of the trigonal prisms about K(1) and K(2) to those in the other channels differ, but the sites have similar sets of two shorter (3.174 to 3.194 Å) plus four longer (3.274 to 3.422 Å) distances to sulfur. Two additional sulfurs are located at 3.977–3.997 Å, distances considerably shorter than the sum of the van der Waals radii, 4.55 Å (9), but slightly longer than metal–metal distances to nearly potassium and indium atoms (Table II). The two shortest potassium–sulfur distances oc-

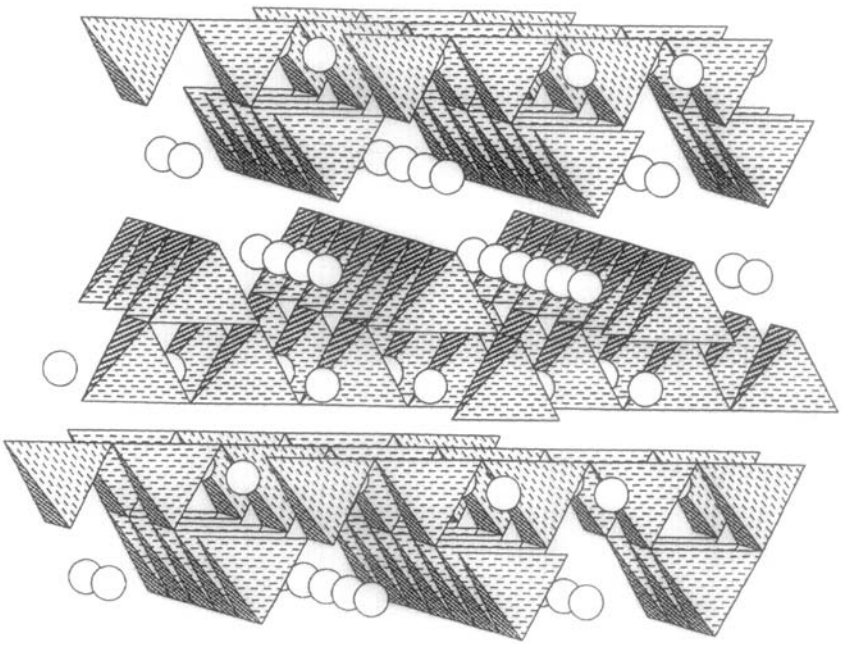

FIG. 3. Polyhedral representation of the layers of vertex-linked $[In_4S_{10}]$ units in $KInS_2$-I. Each layer is rotated 90° relative to neighboring layers. The edges of the large $[In_4S_{10}]$ units in one layer nestle into the channels of the layers above and below, thus completing the trigonal prisms about the potassium atoms.

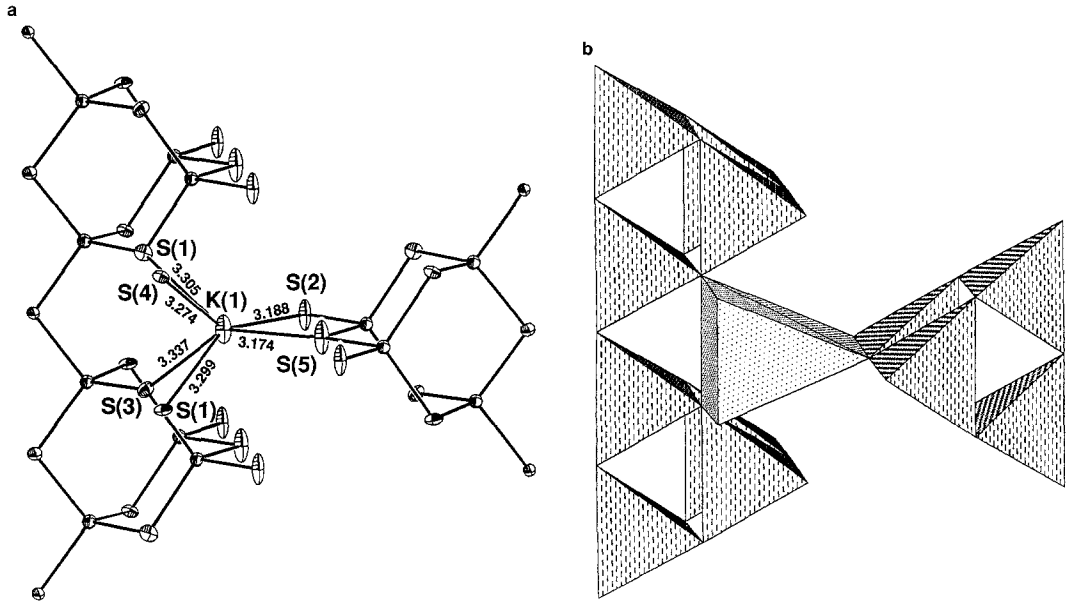

FIG. 4. Views along the channels of potassium atoms showing the interlayer connections in $KInS_2$-I. (a) Ball-and-stick plot with 50% probability ellipsoids and with interatomic distances noted; (b) polyhedral plot.

cur from a potassium in the channel of one layer to sulfurs S(2) and S(5) along the edge of an adjoining layer, thus imparting strong three-dimensional character to the structure. Coordination involving the sulfur atoms in the middle of the layers of $[In_4S_{10}]$ units, S(1), S(3), and S(4), result in potassium–sulfur distances averaging 3.34(5) Å. The K–S bond distances observed in $KInS_2$ are consistent with those observed in other solids: 3.20 Å in K_2S (tetrahedral coordination) (*10*), 3.275 to 3.361 Å in KIn_5S_8 (approximately trigonal prismatic with two additional sulfurs at 3.776 Å) (*11*), and 3.32 to 3.50 Å in $KFeS_2$ (distorted eight-coordination) (*12*).

The In–S distances within the two crystallographically distinct $[InS_4]$ tetrahedra (Table II) range from 2.421 to 2.482(3) Å with a mean value of 2.45(2) Å, and are consistent with the mean distances observed in other compounds containing tetrahedral InS_4 groups; e.g., 2.46 Å in β-In_2S_3 (*13*), 2.50 Å in KIn_5S_8 (*11*), 2.45 Å in $LiInS_2$ (*7*), 2.48 Å in $AgInS_2$ (*14*), 2.48 Å in $Mg_{0.83}In_{2.113}S_4$ (*15*), and 2.47 Å in $BaIn_2S_4$ (*16*). The S–In–S bond angles in $KInS_2$ are slightly distorted from the ideal and range from 105.1 to 113.3(1)°.

The structure contains five crystallographic types of sulfur atoms divided into two structurally similar sets. Half of the sulfur atoms occupy the S(2) and S(5) positions that comprise the string of tetrahedral edges that projects into the potassium channels (see Fig. 4); each of these sulfurs is four-coordinate by two indiums plus two potassiums arranged in a distorted square plane. The other half of the sulfurs occupy the S(1), S(3), and S(4) sites in the middle of the layers of $[In_4S_{10}]$ units and are irregularly six-coordinate by two indium plus four potassium atoms.

Two significant peaks in the difference

TABLE II

BOND LENGTHS (Å) AND BOND ANGLES (DEGREES)[a] IN $KInS_2$-I

In(1)–S(2)	2.448(2)	In(2)–S(1)	2.482(3)
In(1)–S(3)	2.421(3)	In(2)–S(2)	2.447(2)
In(1)–S(1)	2.426(2)	In(2)–S(4)	2.471(2)
In(1)–S(5)	2.439(2)	In(2)–S(5)	2.438(3)
In(1)–K(1)	4.006(2)	In(2)–K(2)	4.010(2)
In(1)–K(2)	3.894(2)	In(2)–K(2)	3.891(2)
K(1)–S(1)	3.305(3)	K(2)–S(1)	3.334(4)
K(1)–S(1)	3.299(3)	K(2)–S(1)	3.422(4)
K(1)–S(2)	3.188(3)	K(2)–S(2)	3.194(3)
K(1)–S(2)	3.992(3)	K(2)–S(3)	3.378(2)
K(1)–S(2)	3.977(3)	K(2)–S(4)	3.379(2)
K(1)–S(3)	3.337(4)	K(2)–S(5)	3.183(3)
K(1)–S(4)	3.274(3)	K(2)–S(5)	3.997(3)
K(1)–S(5)	3.174(3)	K(2)–S(5)	3.986(3)
K(1)–In(1)	4.006(2)	K(2)–In(1)	3.894(2)
K(1)–K(1)	3.948(3)	K(2)–In(2)	4.010(2)
K(1)–K(2)	3.890(3)	K(2)–In(2)	3.891(2)
K(1)–K(2)	3.874(3)		
S(1)–In(1)	2.426(2)	S(3)–In(1)	2.421(3) ×2
S(1)–In(2)	2.482(3)	S(3)–K(1)	3.337(4) ×2
S(1)–K(1)	3.305(3)	S(3)–K(2)	3.378(2) ×2
S(1)–K(1)	3.299(3)		
S(1)–K(2)	3.334(4)	S(4)–In(2)	2.471(2) ×2
S(1)–K(2)	3.422(4)	S(4)–K(1)	3.274(3) ×2
		S(4)–K(2)	3.379(2) ×2
S(2)–In(1)	2.448(2)		
S(2)–In(2)	2.447(2)	S(5)–In(1)	2.439(2)
S(2)–K(1)	3.188(3)	S(5)–In(2)	2.438(3)
S(2)–K(1)	3.992(3)	S(5)–K(1)	3.174(3)
S(2)–K(2)	3.977(3)	S(5)–K(2)	3.183(3)
S(2)–K(2)	3.194(3)	S(5)–K(2)	3.997(3)
		S(5)–K(2)	3.986(3)
S(2)–In(1)–S(3)	109.5(1)	S(1)–In(2)–S(2)	108.9(1)
S(2)–In(1)–S(1)	107.8(1)	S(1)–In(2)–S(4)	111.2(1)
S(3)–In(1)–S(1)	109.1(1)	S(2)–In(2)–S(4)	107.8(1)
S(2)–In(1)–S(5)	105.1(1)	S(1)–In(2)–S(5)	110.9(1)
S(3)–In(1)–S(5)	111.8(1)	S(2)–In(2)–S(5)	105.3(1)
S(1)–In(1)–S(5)	113.3(1)	S(4)–In(2)–S(5)	112.5(1)

[a] Bond angles around the potassium atoms are included with the supplementary material.

Fourier map were modeled and refined as partially occupied indium sites; these sites are translated from positions of In(1) and In(2) by $x = 0.5$. Additional peaks observed in the difference map could arise from other atoms undergoing a similar translation. The slight disorder among indium sites obtained in our refinement may be related to the two stacking arrangements that are possible for the layers of the $[In_4S_{10}]$ units. The second

layer can be translated along the (110) direction (the direction of the potassium chains) by one S–S distance without changing the local coordination environment of any of the atoms. This type of stacking disorder was elegantly described for HgI_2 (*17*), and was also reported for $TlGaSe_2$ (*5*).

Discussion

$TlGaSe_2$ was originally reported in space group *Cc* (*5*); subsequent work indicated that the structure is more correctly described in space group *C*2/*c* (*18, 19*) with transformed atomic coordinates (*18*) very similar to those obtained for $KInS_2$-I in the present study. Other compounds reported to be isostructural with $TlGaSe_2$ and $KInS_2$-I include $KInSe_2$ (*19*); $RbInS_2$-I, $CsInS_2$, $KTlS_2$, $RbTlS_2$, and $CsTlS_2$ (*2*); and $TlAlS_2$, $TlAlSe_2$, $TlGaS_2$, $TlInS_2$, and $RbGaS_2$ (*4*).

The $KInS_2$-I structure bears some similarity to closest-packed-derived structures such as that of HgI_2 (*17*). In the proposed structure for the unstable orange modification of HgI_2 (*17*), the iodine atoms occupy the positions of closet-packing (cp) in a cubic A–B–C sequence. One-fourth of each of the two types of tetrahedral interstices between the layers are equally occupied by the mercury atoms, resulting in layers of vertex-sharing $[Hg_4I_{10}]$ units that are structurally analogous to those comprised of $[In_4S_{10}]$ units in $KInS_2$-I. In the structure of $KInS_2$-I, the cp layers are highly distorted by the covalent nature of the bonding in such a way as to push the layers slightly apart and form the strings of face-sharing trigonal prisms that comprise the channels and accommodate the potassium atoms. A more open structure than that of HgI_2 results, leaving only domains of cubic closest-packing within the layers of $[In_4S_{10}]$ units.

The three-dimensional character of the structure is reflected in the relatively short K–S(2) and K–S(5) bond distances that serve to provide strong interlayer coupling; the $KInS_2$-I crystals are nonmicaceous, water insoluble, and occur as both square platelets and rectangular rods. Furthermore, significant three-dimensional character has also been indicated by Raman data obtained in a study of the isostructural compounds $TlGaS_2$, $TlGaSe_2$, and $TlInS_2$ (*18*); the data were interpreted as indicating a range of interatomic force constants that ruled out a simplified picture of strong intralayer vs weak interlayer bonding.

The unit cell dimensions and density obtained for $KInS_2$-I in the present study differ slightly from those reported by Schubert and Hoppe (*2*); however, those workers refer to the compound as being light red-brown in color, whereas our material is light yellow. Slight sample differences cannot be ruled out, and Ref. (*2*) contains insufficient structural data to examine this question in detail. As few powder patterns have been reported for ambient-pressure $MInS_2$ (M = alkali metal) phases, observed and calculated powder patterns for the structure reported here are listed in Table III.

Conclusions

A single-crystal structure determination of a pale yellow–orange platelet of $KInS_2$-I confirmed that this compound is isostructural with $TlGaSe_2$ (*5*). The structure consists of layers of vertex-sharing $[In_4S_{10}]$ adamantane-like units that are analogous to vapor-phase P_4O_{10}. The stacking of the layers creates channels perpendicular to one another that contain potassium atoms in trigonal prismatic sites. Short interlayer K–S bonding imparts three-dimensionality to the solid.

Acknowledgments

The authors thank Bob Woolever for the SEM/EDX analyses. D.O.K.'s postdoctoral fellowship was administered by the American Society for Engineering Education. This work was supported by the Office of Naval Research.

TABLE III

CALCULATED AND OBSERVED POWDER PATTERNS FOR $KInS_2$

Pattern calculated from single-crystal structure determination[a]						Observed film data[b]	
h	k	l			d-spacing calculated	I_{rel}	d-spacing observed	I_{obs}
1	1	0			7.6976	4		
0	0	2			7.3781	30	7.38	50
−1	1	1			7.2224	24		
1	1	1			6.4864	38	6.47	20
−1	1	2			5.7120	33	5.71	10
1	1	2			5.0098	17	5.03	5
−1	1	3			4.4146	4	~4.44	2
−2	2	1	(2 2 0)		3.8489	24	3.84	40
0	0	4			3.6891	19	3.71	40
−2	2	2	(2 2 1)		3.6112	75	3.62	80
−3	1	1	(1 3 0)		3.4665	31	3.46	40
3	1	0	(−1 3 1)		3.4195	17		
−3	1	2	(1 3 1)		3.3315	3		
−2	2	3	(2 2 2)		3.2436	3		
1	1	4			3.1694	4		
−3	1	3	(1 3 2)		3.0691	15	3.046	2
−1	3	3	(3 1 2)		2.9150	29		
−1	1	5			2.8844	4		
−2	2	4	(2 2 3)		2.8560	100	2.850	100
−3	1	4	(1 3 3)		2.7585	34	2.760	5
−4	0	2	(4 0 0)	etc.	2.6990	4		
−1	3	4	(3 1 3)		2.6035	25	2.596	5
3	3	0			2.5659	3		
−3	3	2			2.5281	5	~2.526	1
3	3	1			2.4740	5	2.456	5
−3	1	5	(−4 2 1)	etc.	2.4555	11		
−3	3	3			2.4075	3		
−5	1	1	(1 5 0)		2.1521	11	2.145	10
−5	1	2	(−1 5 1)		2.1408	5		
−1	1	7			2.1044	3		
−1	3	6	(3 1 5)		2.0638	4		
5	1	1	(1 5 2)		2.0459	5		
−4	0	6	(0 4 5)	etc.	2.0103	49	2.007	60
−5	1	4	(−1 5 3)		1.9987	9		
1	1	7			1.9687	4		
−2	2	7	(2 2 6)		1.9598	7		
−3	1	7	(1 3 6)		1.9526	7		
5	1	2	(1 5 3)		1.9456	10		
−4	4	1			1.9410	39	1.9412	50
−5	1	5	(−1 5 4)		1.8893	7	~1.8878	1
−4	4	3	(4 4 1)		1.8772	4		
5	3	0	(−3 5 2)		1.8596	3		
−1	3	7	(3 1 6)	etc.	1.8499	12	~1.8423	5
−5	3	3	(3 5 1)		1.8379	4		
5	1	3	(1 5 4)		1.8299	3		
5	3	1	(−3 5 3)		1.8099	2		
−3	1	8	(1 3 7)	etc.	1.7561	11	1.7502	5

TABLE III—*Continued*

Pattern calculated from single-crystal structure determination[a]						Observed film data[b]	
h	k	l		d-spacing calculated	I_{rel}	d-spacing observed	I_{obs}
1	1	8		1.7429	3		
−6	2	2	(−6 2 1) etc.	1.7332	4		
−4	4	5	(4 4 3)	1.7179	8		
−6	2	3	(6 2 0) etc.	1.7098	18	1.7117	10
−4	0	8	(0 4 7) etc.	1.6721	11	1.6695	10
−1	3	8	(3 1 7) etc.	1.6695	3		
−6	2	4	(6 2 1) etc	1.6655	2		
−5	1	7	(−1 5 6) etc.	1.6492	3		
−6	2	5	(6 2 2) etc.	1.6055	27	1.6052	20
			(1 5 6) etc.				
5	1	5		1.5906	3		
−2	2	9	(2 2 8)	1.5849	7	1.5853	10
−7	1	3	(5 5 0) etc.	1.5397	3		
−5	1	8	(−1 5 7) etc.	1.5343	5		
		0	(−5 5 3) etc.				
7	1			1.5272	3	~1.522	1
−4	4	7	(4 4 5)	1.5238	2		
5	1	6	(1 5 7)	1.4791	2		
0	0	1		1.4756	4	1.4742	5
−2	2	1	(2 2 9) etc.	1.4417	2		
−5	3	8	(3 5 6) etc.	1.4269	3	~1.4371	1
−3	5	8	(5 3 6)	1.3823	2		
−6	2	8	(−2 6 7) etc.	1.3793	4		
−7	3	5	(−3 7 4)	1.3743	3		
−8	0	2	(0 8 0)	1.3726	10	1.3717	5
7	3	2	(3 7 3)	1.3537	2		
−2	6	8	(−6 2 9) etc.	1.3018	3	~1.2990	2
8	0	2	(−8 0 6) etc.	1.2864	2		
−6	6	3	(6 6 0) etc.	1.2830	2		
−6	6	5	(6 6 2)	1.2371	5	~1.2411	1
−7	5	5	(5 7 2)	1.2289	2		
−6	2	10	(−2 6 9) etc.	1.2276	5	1.2289	2
−2	2	12	(2 2 11)	1.2184	2	1.2177	1
−4	0	12	(0 4 11) etc.	1.2052	3		
7	3	5	(3 7 6) etc.	1.2034	3	1.2046	2
−4	4	11	(4 4 9)	1.1748	6	1.1753	5
−9	3	2	(−3 9 1) etc.	1.1574	2	1.1593	2
−4	8	6	(−8 4 7) etc.	1.1334	10	1.1318	5

[a] The calculated powder pattern of $KInS_2$ in $C2/c$ does not include the disordered indium atoms from the refinement; d-spacing values are calculated from the unit cell parameters $a = 10.981$, $b = 10.979$, $c = 15.010$ Å, $\beta = 100.55°$ for Cu$K\alpha$, $\lambda = 1.5418$ Å. Intensities were calculated as equal to $F^*F^*Lp^*$mult (scaled to 100); intensities were then summed (additively) for overlapping lines. I_{rel} are the summed intensities renormalized to a scale of 0 –100. Most lines with $\Sigma I < 4.0$ (before renormalization) are not listed.

[b] The observed Debye–Scherrer film datas for (crushed) yellow platelets of $KInS_2$ were recorded in a camera of diameter 114.6 mm with nickel-filtered copper radiation.

References

1. D. O. Kipp, C. K. Lowe-Ma, and T. A. Vanderah, *Chem. Mater.* **2,**(5), 506 (1990).
2. H. Schubert and R. Hoppe, *Z. Naturforsch.* **25b,** 886 (1970).
3. K. J. Range and G. Mahlberg, *Z. Naturforsch.* **30b,** 81 (1975).
4. D. Müller, F. E. Poltmann, and H. Hahn, *Z. Naturforsch.* **29b,** 117 (1974).
5. D. Müller, and H. Hahn, *Z. anorg. allg. Chem.* **438,** 258 (1978).
6. S. K. Kovach, E. E. Semrad, Yu. V. Voroshilov, V. S. Gerasimenko, V. Yu. Slivka, and N. P. Stasyuk, *Inorg. Mater.* **14,** 1693 (1978).
7. Z. Z. Kish, E. Yu. Peresh, V. B. Lazarev, and E. E. Semrad, *Inorg. Mater.* **23,** 697 (1987).
8. SHELXTL PC, Version 4.1, Siemens Analytical X-Ray Instruments (May 1990).
9. A. Bondi, *J. Phys. Chem.* **68,** 441 (1964).
10. R. W. G. Wyckoff, "Crystal Structures," 2nd ed. Vol. 1, p. 242, Wiley–Interscience, New York (1963).
11. D. Carré and M. P. Pardo, *Acta Crystallogr. Sect. C* **39,** 822 (1983).
12. W. Bronger, *Z. anorg. allg. Chem.* **359,** 225 (1968).
13. G. A. Steigmann, H. H. Sutherland, and J. Goodyear, *Acta Crystallogr.* **19,** 967 (1965).
14. H. Hahn, G. Frank, W. Klingler, A.-D. Meyer, and G. Störger, *Z. anorg. allg. Chem.* **271,** 153 (1953).
15. B. Eisenmann, M. Jakowski, and H. Schäfer, *Mater. Res. Bull.* **19,** 77 (1984).
16. B. Eisenmann, M. Jakowski, W. Klee, E, and H. Schäfer, *Rev. Chim. Minérale* **20,** 255 (1983).
17. D. Schwarzenbach, *Z. Kristallogr.* **128,** 97 (1969).
18. W. Henkel, H. D. Hochheimer, C. Carlone, A. Werner, S. Ves, and H. G. v. Schnering, *Phys. Rev. B* **26,** 3211 (1982).
19. B. Krebs, *Angew. Chem. Int. Ed. Engl.* **22,** 113 (1983).